Design of high-speed interior permanent magnet-type motor for turbo machinery**

Yohji Okada,* Fumiya Kitayama and Ryou Kondo

School of Engineering, Ibaraki University, 3-14-6 Nakanarusawa, Hitachi 316-8511, Japan

A high speed interior permanent magnet (IPM)-type motor is proposed. It is intended for application to high speed turbo-machinery supported by magnetic bearings. Such a system usually calls for a big uninterruptible power supply (UPS) to support the rotor when the power supply stops suddenly. The proposed motor generates electric power from the rotational energy when the power suddenly ceases. The regenerated energy is used to operate the magnetic bearing until the rotor speed slows down. The rotor touches down to the emergency ball bearing. This high speed IPM-type motor easily regenerates the electric energy with diodes only, which can replace the big UPS. This paper proposes a two-pole IPM motor as a generator for such a sudden power interruption. For high speed rotation, a two-pole IPM motor is fabricated and tested.

Keywords: high-speed motor, magnetic bearing, regenerative energy

1. Construction of proposed motor

Analytical models of two-pole IPM-type motors[1] were analysed. The motors are expected to run up to 20,000 rpm. The original analytical models are shown in Fig. 1. The standard 6-slot type is shown on the left, and a modified 12-slot one is shown on the right. The motor yoke is made from thin nonoriented electrical steel sheet (15HX1000) with an outer diameter of 100 mm.

As mentioned later, the 6-slot type produces high torque, but cannot run up to a high speed. We decided to test the 12-slot type, which has a special coil arrangement. Each stator pole has two windings: the upper top pole has two U coils, the right next one has U and W coils, and the 60° right one has two –W coils, and so on for a smooth flux distribution. The rotor scheme is shown in Fig. 2. Inside the rotor six permanent magnets (PMs) (Shin-Etsu N32EX) were inserted in two lines to give N–S polarities. The detailed dimensions were determined using the commercial finite element method (FEM) MagNet software.

* Corresponding author. E-mail: yohji.okada.spam@vc.ibaraki.ac.jp

** This paper was first presented at the eleventh Japanese–Mediterranean workshop (JAPMED'11), 15–19 July 2019 in Batumi, Georgia.

1 Okada, Y., Kitayama, F. & Kondo, R., Proposal of high speed IPM motor for turbo machinery supported by magnetic bearings, *Proc. MAGDA2018 Conference*, pp. 74–77. Katsushika, Tokyo, 20–21 October 2018 (in Japanese).

Nanotechnology Perceptions **15** (2019) 227–237
Received 6 September 2019; *accepted* 30 November 2019

doi: 10.4024/N25OK19A.ntp.15.03

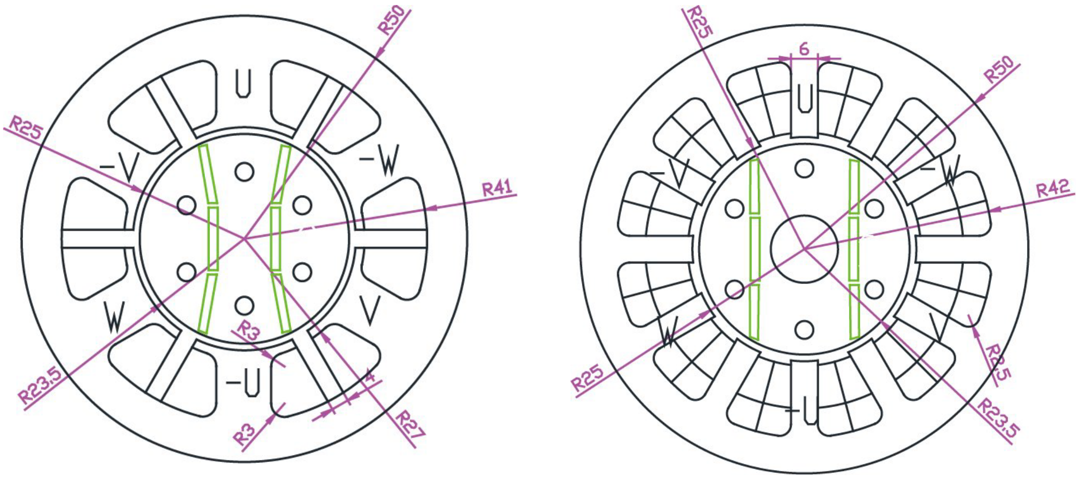

Figure 1. Analytical model of the IPM high-speed motor (left: 6-slot; right 12-slot). Length unit is mm.

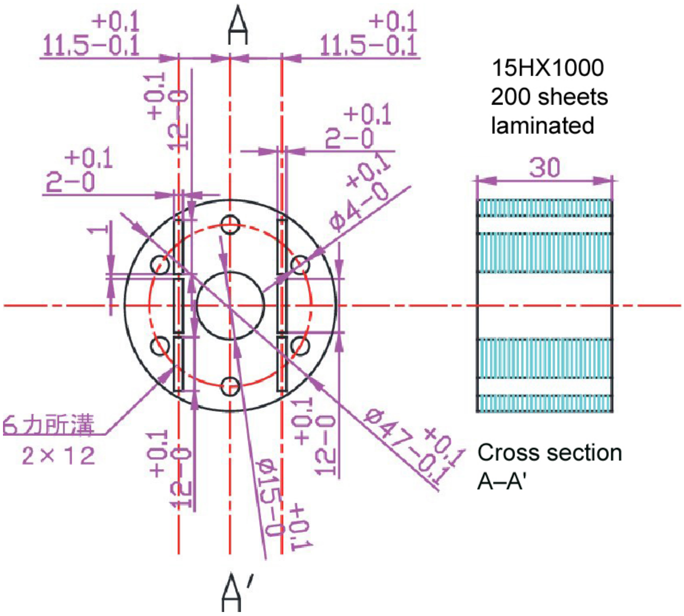

Figure 2. Schematic construction of the IPM rotor (length unit is mm).

The coils were wound by a hand-winding machine, as shown in Fig. 3. The magnet wire used has a diameter of 0.6 mm. The measured coil characteristics are shown in Table 1.[1] The upper and lower coils are of different types. But the resistance, inductance and flux density at 1 A coil current are almost the same. These coils were inserted in the stator poles; the upper pole had coil #1 and #13, the right next one had coil # 2 and #14 and so on, as shown in Fig. 4. After testing the motor run, the rotor speed was not high. Then, the stator was modified *qua* the closed slot pole. The tops of the stator slots were connected by thin magnetic soft iron (SUY-1) with a thickness of 0.7 mm.

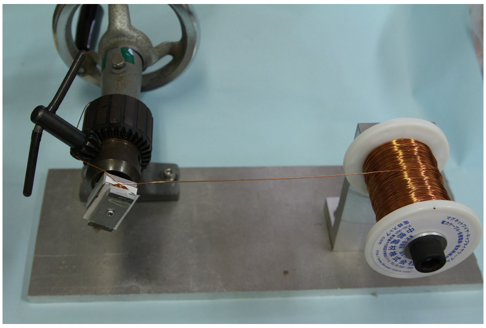

Figure 3. Scheme of hand-made coil windings.

Table 1 Coil characteristics for each slot.

Coil Characteristics (Outer, ϕ0.6, 42turn)												
Coil #	1	2	3	4	5	6	7	8	9	10	11	12
R [mΩ]	268	261	245	245	246	249	256	250	234	242	243	265
L [μH]	347	365	339	346	343	365	365	360	317	331	332	330
B [mT/A]	8.5	8.5	7.5	8	8.5	9	9	9	9	7.5	8	7.5
Coil Characteristics (Inner, ϕ0.6, 42turn)												
Coil #	13	14	15	16	17	18	19	20	21	22	23	24
R [mΩ]	360	238	233	230	227	233	249	244	247	252	246	238
L [μH]	222	224	199	217	194	223	241	232	237	236	215	224
B [mT/A]	7.5	7.5	8.5	8.5	9	7.5	8.5	8.5	9	8.5	8.5	8.5

Figure 4. Photograh of closed slot stator.

2. Fabricated motor and FEM analytical results

Fig. 5 shows the bias flux distribution analysed by FEM software MagNet. The bias flux is well formed except for the narrow stator yoke path. Next, the torque versus motor speed characteristics were calculated by giving a 4 A peak sinusoidal current to the three phase U, V and W coils, as shown in Fig. 6. The supply voltage is 72 V. There are three curves, for the 6-slot, 12 open slot and

12 closed slot types. The 6-slot type motor has a simpler construction and produces a higher torque, but the top speed is limited to 10,000 rpm. The 12 open slot type can achieve high speed, but the cogging torque is bigger. As mentioned later, the open slot type does not rotate well up to high speed. We changed the stator by connecting the top of neighbouring stator poles with thin soft magnetic iron (SUY-1) to reduce the cogging torque, as shown in Fig. 4. The 12-slot motor can run at over 20,000 rpm, from the analytical results in Fig. 6. The low-speed torques are shown in Fig. 7, where the upper curve is for the open slot type and lower one for the closed slot type. Rotation at 2 rpm needs 500 ms for 360° rotation. Hence, Fig. 7 shows the torque during one rotation. The figure shows that the average rotating torques are almost the same, while the closed slot cogging torque is about half compared with the open slot type. The assembled rotor and stator are shown in Fig. 8.

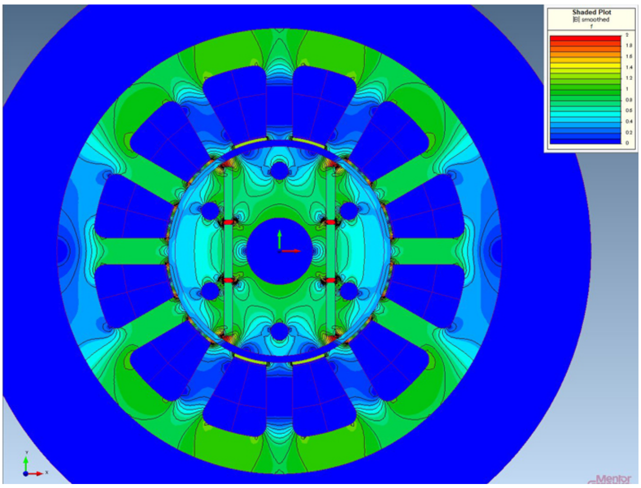

Figure 5. Calculated bias flux using MagNet.

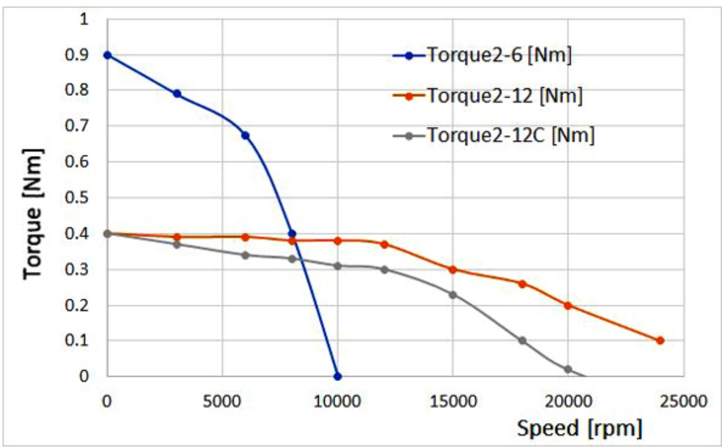

Figure 6. Torque versus speed curves (72 V).

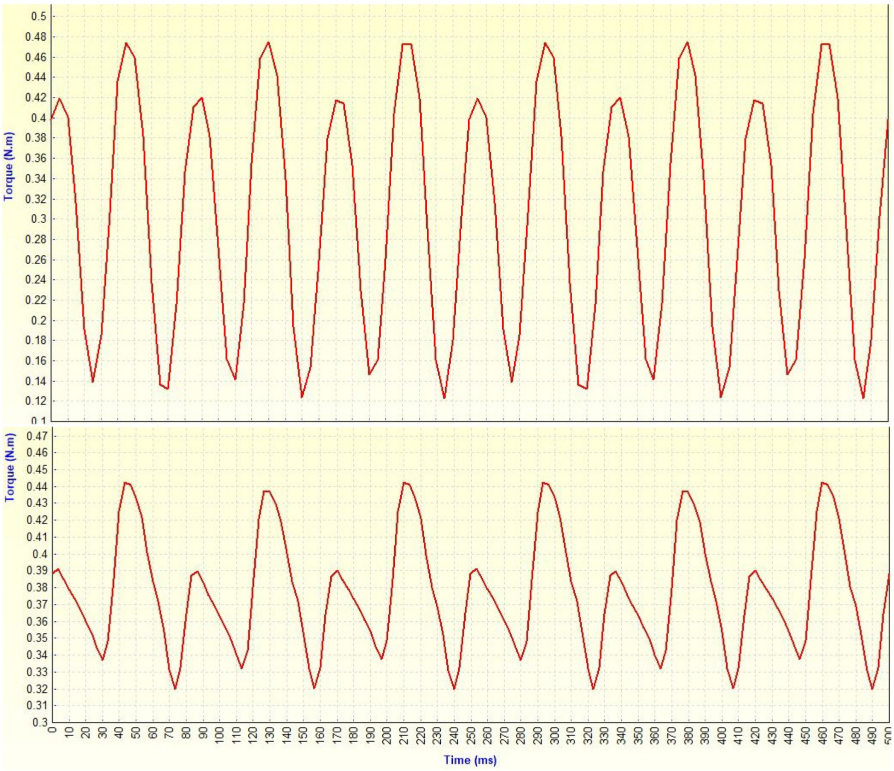

Figure 7. Low-speed cogging torque calculation at 2 rpm (upper panel: open slot; lower panel: closed slot).

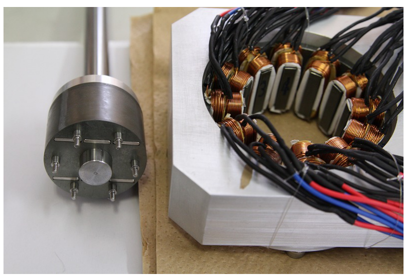

Figure 8. The assembled rotor and stator (open slot type).

3. Back electromotive (BEM) voltage test

The fabricated motor was driven by an external d.c. motor (Maxon 148877) and the BEM voltage test carried out as shown in Fig. 9. The three-phase BEM voltage (U, V, W phase voltages) was measured at a rotation speed of 3,000 rpm. Results are shown in Fig. 10 for the open and closed slot motor types. There is high-frequency ripple, but we can recognize the fundamental frequency components. The closed slot one has about half the cogging torque and the rotating torque is almost the same. Testing the motor shaft by hand rotation, one feels a relatively smooth rotational resistance.

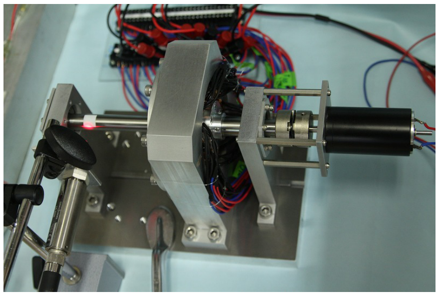

Figure 9. Photo of BEM test driven by a d.c. motor.

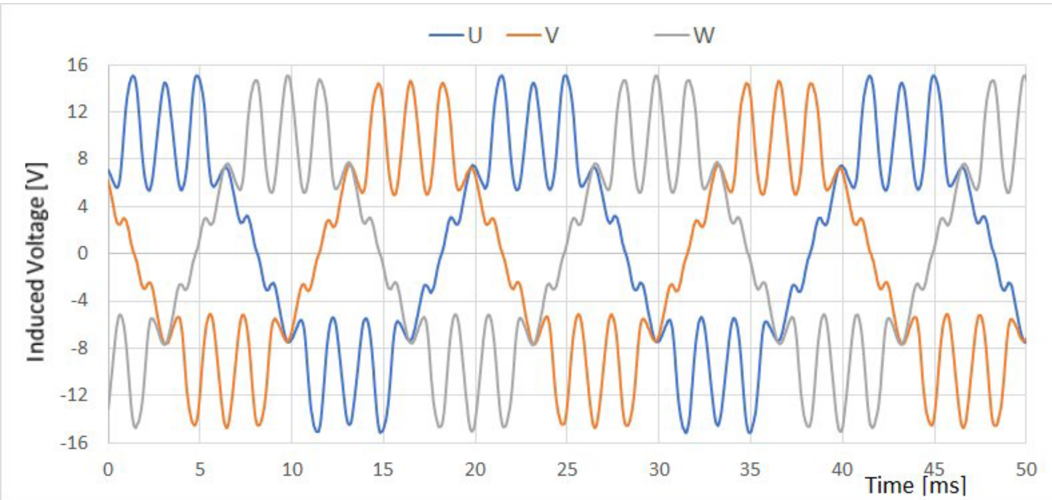

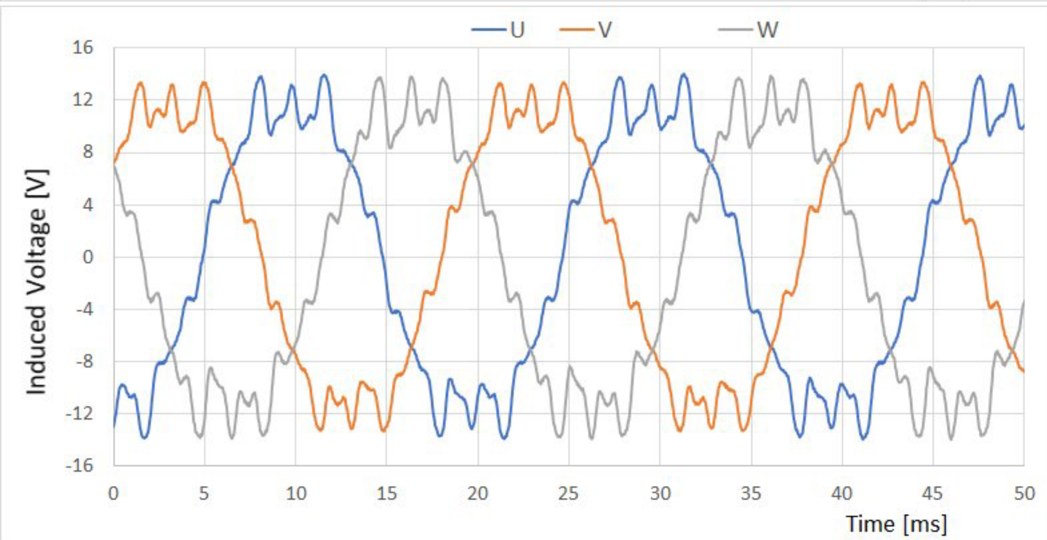

Figure 10. BEM test results of the 12-slot motors (upper, open slot; lower, closed slot).

4. No-load motoring test

Firstly, the 12-open slot motor was tested by the synchronous motor controller. The dSPACE model of the motor controller is shown in Fig. 11. The analog driving signals are sent to three single phase PWM power amplifiers (Copley Co., model 4212Z) to drive the motor. However, the motor rotation was stopped above 1,000 rpm. For realizing high-speed rotation, the stator was modified to a closed slot-type one and rotor angle was measured by an encoder (Omron E6D). The encoder was attached to the motor shaft as shown in Fig. 12 and the encoder pulses were put into the counter on dSPACE, as shown in the left of Fig. 13. According to the rotor angle, a servo controller was installed in dSPACE to drive the motor as 90 degree electric angle advanced, which is also shown in Fig. 13. The encoder pulse was put into an F/V converter (JRC NJM4151D) separated from dSPACE to get the analog rotor speed voltage. This rotating speed voltage was connected to an A/D converter (right upper corner of Fig. 13). The top left (constant) was the reference speed signal and the error signal is put into the PID controller to control the magnitude of the three-phase (U, V, W) sinusoidal signals. The PI control gains used were P=2.0, I=20 and D=0 in Fig. 13. No-load rotation was achieved up to 12,000 rpm. Example waves at 8,000 rpm are shown in Fig. 15. These waveforms show relatively balanced currents. But at 12,000 rpm the currents include higher components and vibration, which is considered to arise from mechanical weakness of the motor system.

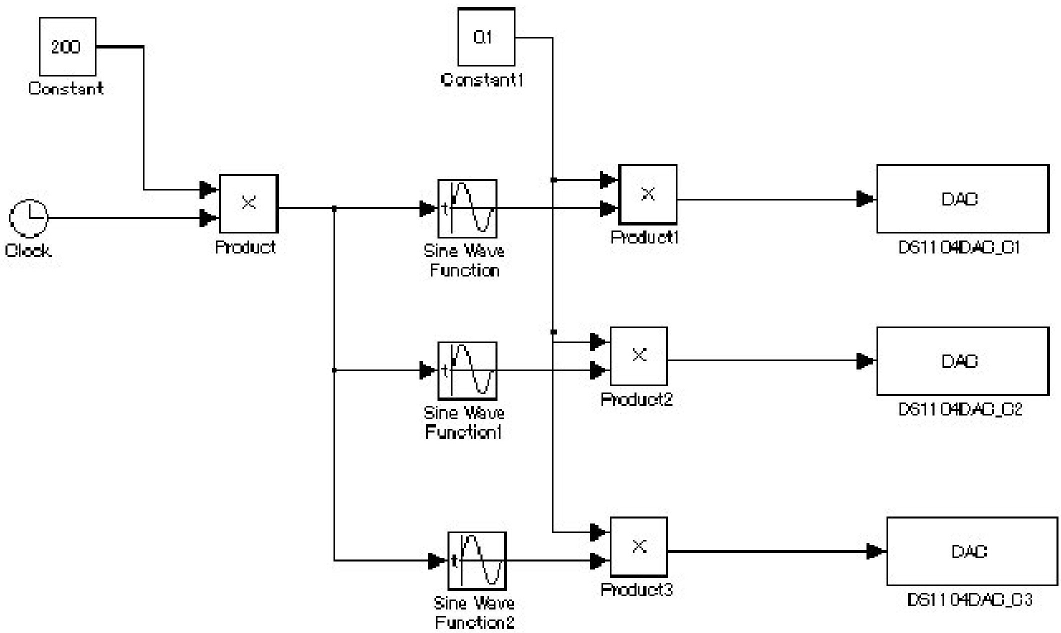

Figure 11. Synchronous motor controller installed in dSPCE (DS-1104).

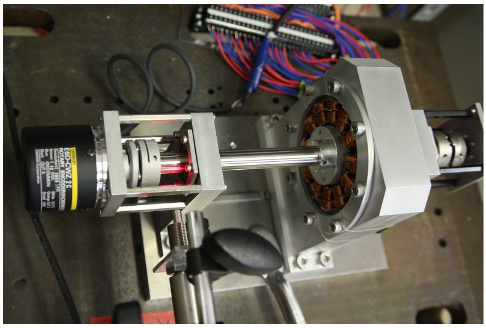

Figure 12. An encoder is attached to the shaft of the motor for high-speed rotation.

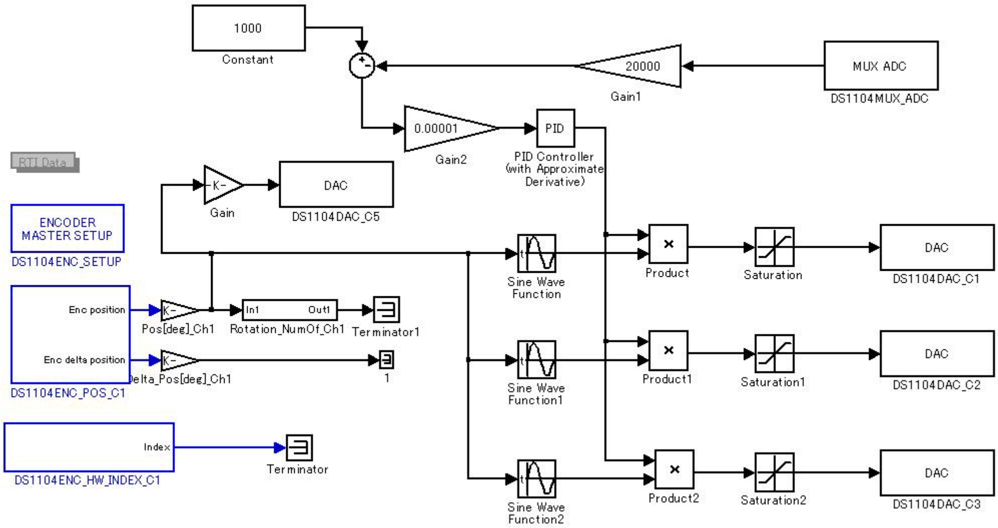

Figure 13. Servo motor controller for the dSPACE model (DS-1104). Please refer to the main text for more explanation.

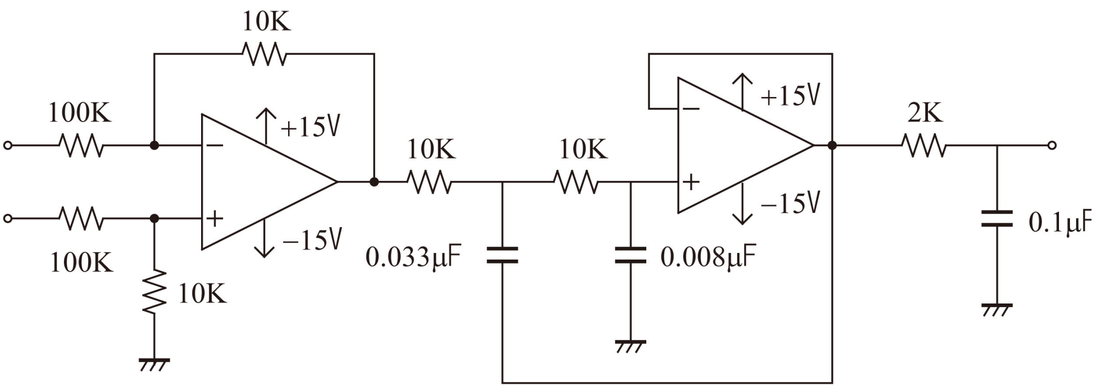

Figure 14. Anti-aliasing filter for measuring PWM driving voltage.

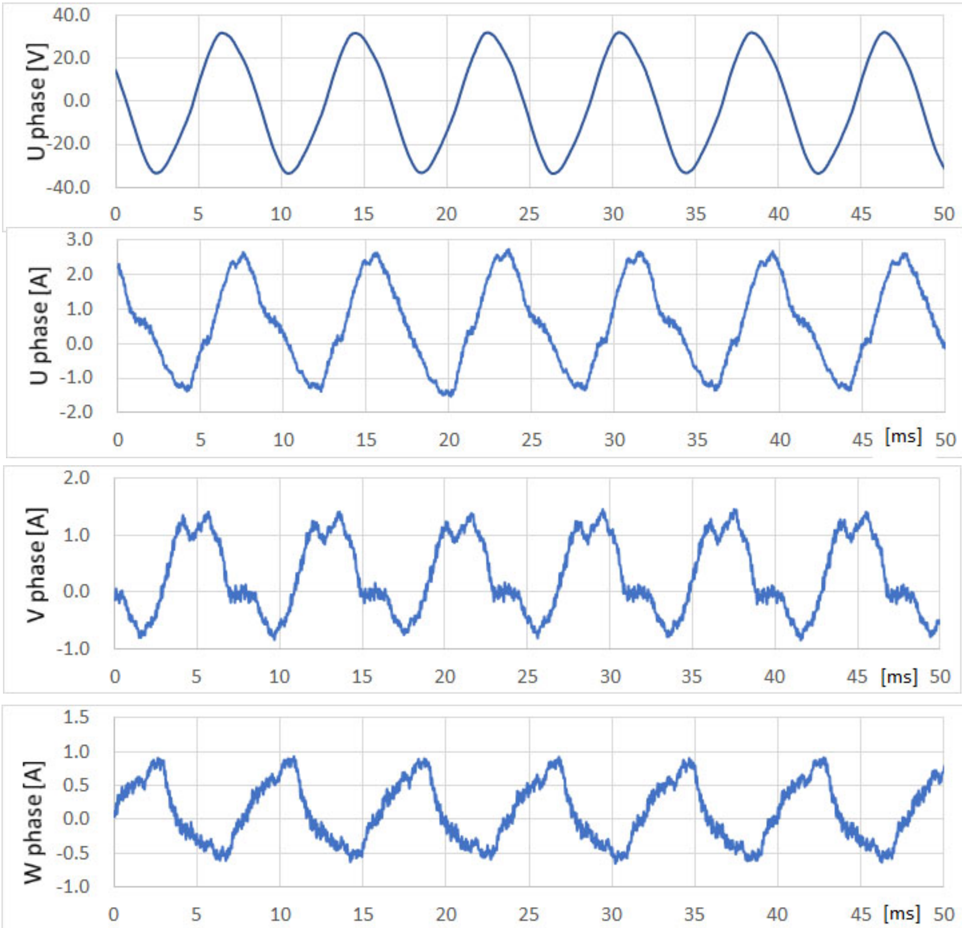

Figure 15. Measured driving voltage (top: U, phase voltage), and the three phase currents (below) U, V and W at 8,000 rpm.

5. Loaded motor test

The loaded motor test was carried out using a Sugawara PC-SAA2, TB-2KS motor analyser and a Yokogawa WT1600 power meter (Fig. 16). The motor was driven by the same servo motor controller as in the previous section. As mentioned before, rotation up to 8,000 rpm was relatively stable. The measured loaded characteristics are shown in Fig. 17. The supply voltage was 72 V, the power amplifier was almost saturated. The reference speed was 8,000 rpm, but the loaded motor speed (blue line) decreased according to the load torque from the motor analyser. The output power (orange line) increased almost linearly with load torque. The motor efficiency (grey line) was about 60% between 100 and 200 mNm load torque, and the maximum efficiency was 65%. However, the loaded motor could not run at a higher speed due to the voltage limit. According to the technical specification of the power amplifier (Copley Co., 4212Z), the maximum supply voltage is 120 V, but over 72 V it produced some distortion in the current waves.

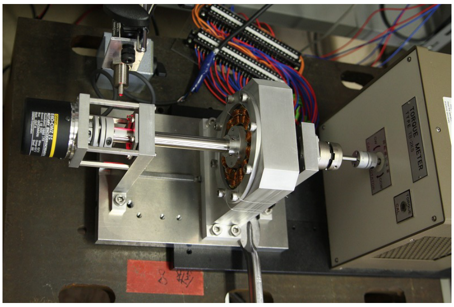

Figure 16. The developed motor being tested by a motor analyser giving the load torque.

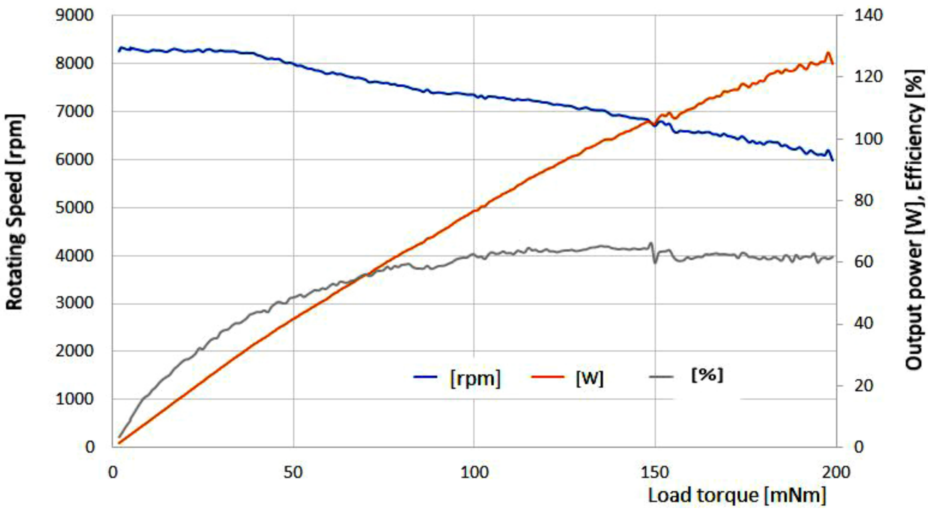

Figure 17. Rotation speed, output power and motor efficiency with increasing load torque.

Several organizations are developing a high-speed motor driver, for example the Japan Aerospace Exploration Agency (JAXA)'s high-speed motor driver for a space robot.[2] Due to budget limitations we could not use a better motor driver.

6. Conclusions and proposed future work

A two-pole high-speed motor has been proposed. It was fabricated and tested. The top speed is recorded up to 12,000 rpm. A loaded motor test was carried out using a motor analyser up to 8,000 rpm. The maximum efficiency recorded was 65%, which is quite good for a two-pole type IPM motor for high-speed applications and for regenerative operation when the electric power is suddenly interrupted.[3]

---

2 Asama, J. & Noguchi, T., A 7-level pseudocurrent source inverter for high-speed motor applications. *Proc. 31st Symposium on Electromagnetics and Dynamics*, paper 23A4-3 (CD-ROM). Tokyo Institute of Technology, Suzukakedai campus, 22–24 May 2019 (in Japanese).

3 Schweitzer, G. & Maslen, E.H. (eds), *Magnetic Bearings*, pp. 1–406. Springer (2009).

Further research work is continuing on supporting one end of the shaft by a magnetic bearing, which has been previously developed.[4] Increasing the top speed of the motor will be investigated, and the consequences of interrupting the electricity supply will be tested. We shall use the proposed motor as the generator. The regenerated energy will be used to supply the magnetic bearing. As rotation slows down the shaft will be tested for safely touching down to the emergency ball bearing.

Acknowledgment

The research is supported by the Tsugawa Foundation, to which the authors would like to express their sincere appreciation.

---

[4] Okada, Y., Suzuki, H., Matsuda, K., Kondo, R. & Enokizono, M., Development of highly efficient magnetic bearing to ultra-low temperature fluid pump. *Bull. JSME Mech. Engng J.* **2(4)** (2015) 1–10 .